Oblique shocks in rapid granular flows

Kristin Martha Hákonardóttir
Centre for Environmental and Geophysical Flows, School of Mathematics, University of Bristol, Bristol BS8 1TW, United Kingdom and Icelandic Meteorological Office, Bústadavegur 9, IS-150 Reykjavik, Iceland

Andrew J. Hogg[a)]
Centre for Environmental and Geophysical Flows, School of Mathematics, University of Bristol, Bristol BS8 1TW, United Kingdom

(Received 4 November 2004; accepted 23 May 2005; published online 1 July 2005)

The interaction between rapid, free-surface granular flows and deflecting dams is investigated by laboratory experimentation and by the formulation and analysis of a shallow-layer model of the motion. It is found that uniform, downslope flows of grains are deflected to flow parallel to the barrier and that upstream of the barrier, the flow state undergoes an abrupt transition whereby its depth, velocity, and direction of motion change. These oblique shocks are investigated for a range of Froude numbers and for a range of angles between the deflector and the direction of steepest descent. The experimental results are found to be in good agreement with predictions from the shallow-layer theory. Experiments were also conducted with rapid, free-surface flows of water. They reveal not only similarities between the steady deflection patterns of the water and grain flows, but also some differences in the nature of their initial interaction. A simple interpretation for this is given in terms of the relatively high pressures that develop during the initial impact of the incompressible water with the impermeable barrier. Deflecting dams are deployed to defend against large-scale snow avalanches and these results are applied to this situation. © *2005 American Institute of Physics*. [DOI: 10.1063/1.1950688]

I. INTRODUCTION

Granular media are ubiquitous. In industry, many chemical and food products are processed in a particulate form, while in nature, the morphology of the environment is often shaped by intense two-phase flows. Large-scale granular flows may also pose significant natural hazards. They may flow rapidly and transport very large volumes of disaggregated solids over long distances. For example, rockfalls and snow avalanches may attain speeds of over 50 m s^{-1} and may consist of volumes of many cubic kilometers of particulate material.[1,2] Despite these varied and important examples of granular flows, the dynamics of these materials remain poorly understood at a fundamental level and there is considerable current interest in elucidating their properties.[3]

Rapid free-surface flows of cohesionless grains have been a focus of study during recent years not just because they constitute one of the generic flows, but also because understanding these flows has a direct application to many environmental phenomena. Some notable contributions include the analytical study of Savage and Hutter,[4] who derived a theoretical model based on the shallowness of the flowing layer and the assumption that the material was a cohesionless, Mohr-Coulomb continuum that slipped at the base; Johnson *et al.*,[5] who studied chute flows experimentally and deduced empirically a law that included the stresses due to frictional and collisional interactions between the particles; and more recently, Pouliquen[6] has performed experiments and proposed a new model of steady flows of particles down a roughened plane.

A key feature of many granular flows is that they are sufficiently rapid so that the inertia of the motion cannot be neglected. Therefore, in common with supercritical free-surface flows of water and supersonic flows of gas, we expect that the flow may undergo almost discontinuous transitions between flow states (bores and hydraulic jumps/shocks) and that the general characteristics of these transitions are relatively insensitive to the resistive and dissipative processes. Furthermore, in terms of the mathematical models of these flows, we anticipate that the systems of governing equations are hyperbolic so that discontinuous solutions and other transitions are admissible. Shock-like structure in granular materials have been reported before. For example, in experiments performed with a confined, single layer of particles, Horlück and Dimon[7] found shock waves in the motion through a constriction, and Rericha *et al.*[8] identified shock-like transitions when the flow is deflected obliquely by an obstacle. Samadani *et al.*[9] found jumps in the free surface of silo flows. Finally, for free-surface flows, Savage[10] and Brennen *et al.*[11] found "granular jumps" that are hydraulic jumps normal to the direction of flow, while Gray *et al.*[12] found normal and oblique shocks when the flow is deflected by an obstacle. These latter experiments share some features with those reported below, although the interpretation of the results is somewhat different; they will be discussed further in Sec. III. Shocks and other transitions have been analyzed theoretically by many investigators.[13–15] Furthermore, they

[a)]Electronic mail: a.j.hogg@bris.ac.uk

have been simulated computationally for flows around submerged cylinders[16] and wedges.[17]

In this paper, we investigate experimentally and theoretically the lateral deflection of free-surface, rapid granular flows by stationary obstacles. This work is partly motivated by its application to barriers that are built to defend against snow avalanches. Such deflecting dams turn the oncoming flow away from mountainous villages that lie in the avalanche path. Current understanding of the mechanics of the deflection process is limited and so design criteria, such as those given in McClung and Schaerer,[17] lack theoretical foundation. This work, therefore, provides significant new insights into the interaction between the flow and the obstacle, and may be used to reformulate design guidelines. (See the works by Hákonardóttir, Hogg, Batey, and Woods,[18] and Hákonardottir, Hogg, Jóhannesson, and Tómasson[19] for studies of the interactions between other types of avalanche defense structures and rapid flows.)

Our purposes in this study are twofold. First, we aim to investigate more thoroughly the steady deflection of granular flows by obstacles and to establish a theoretical model of the interaction that may predict quantitatively the flow following deflection. We will also establish the characteristics of the initial, transient impact of the flow against the obstacles. In addition, we elucidate those features that are in common, and those that differ, between rapid flows of water and of grains. In this way, we determine some of the mechanical properties of these rapid granular flows and identify some of the phenomena that complete theories of the flow of such materials must predict.

The paper is organized as follows. We formulate a reduced, shallow-layer model of the flow in Sec. II, and review the assumptions that underlie it and the relationships that must hold across discontinuities in the flow. This analysis highlights the importance of the upstream Froude number of the flow, F, in determining the nature of the deflection. We derive these properties in the regime $F \gg 1$, which corresponds to the flow regime of many natural avalanches.[2] We then describe the experimental series (Sec. III A) and present the results of the experiments (Sec. III B). We also analyze the differences in the behavior of the initial impact on the obstacle of water and grains flows, and present a new model of the splash height (Sec. III C). In addition, we discuss the development of the flow along the dam (Sec. III D). Finally, we draw some conclusions and discuss their implications for avalanche defense structures (Sec. IV).

II. DEPTH-AVERAGED MODEL

The granular material flows down a rigid plane, inclined at an angle θ to the the horizontal. We align the coordinate axes such that the z axis is perpendicular to the plane, the x axis is parallel to the direction of steepest descent, and the y axis is perpendicular to these two. The depth and bulk density of the flowing layer of grains are denoted by h and ρ, and thus conservation of mass is given by

$$\frac{\partial}{\partial t}\int_0^h \rho\, dz + \frac{\partial}{\partial x}\int_0^h \rho u\, dz + \frac{\partial}{\partial y}\int_0^h \rho v\, dz = 0, \tag{1}$$

where u and v are the components of the velocity field along the x and y axes, respectively.

The depth of the flow is assumed to be much less than the lengthscales over which the flow varies in the plane. This implies that vertical accelerations are negligible and the vertical momentum equation is considerably simplified. Denoting the pressure tensor by p_{ij}, this implies that to leading order

$$p_{zz} = \int_z^h \rho g \cos\theta\, d\eta, \tag{2}$$

where it has been further assumed that the upper surface of the flow is stress-free. The momentum equations parallel with the plane are then given by

$$\frac{\partial}{\partial t}\int_0^h \rho u\, dz + \frac{\partial}{\partial x}\int_0^h \rho u^2 dz + \frac{\partial}{\partial y}\int_0^h \rho uv\, dz = -\frac{\partial}{\partial x}\int_0^h p_{xx} dz - \frac{\partial}{\partial y}\int_0^h p_{xy} dz - \tau_x + \int_0^h \rho g \sin\theta\, dz, \tag{3}$$

$$\frac{\partial}{\partial t}\int_0^h \rho v\, dz + \frac{\partial}{\partial x}\int_0^h \rho uv\, dz + \frac{\partial}{\partial y}\int_0^h \rho v^2 dz = -\frac{\partial}{\partial x}\int_0^h p_{xy} dz - \frac{\partial}{\partial y}\int_0^h p_{yy} dz - \tau_y. \tag{4}$$

In these expressions the basal shear stress has components τ_x and τ_y, which are equal to p_{xz} and p_{yz} evaluated at the boundary $z=0$. We note that in this mathematical model, the momentum of the interstitial fluid is neglected along with the interaction between it and the granular material.

To close this mathematical model of the motion, we make a series of further assumptions. First, we assume that the bulk density of the flowing material is uniform. Although granular materials must dilate in order to flow, once mobilized, their bulk density often varies only negligibly.[4,12,20] Thus, we treat the material as incompressible. In addition, we assume that the velocity fields u and v are vertically uniform; such an assumption underlies most depth-averaged, hydraulic models of river, estuarine, debris, and avalanche flows. In general, the neglect of the vertical structure introduces little error in the modeling (although see the work by Hogg and Pritchard[21] for a notable exception). Current understanding of the wide range of dynamical behaviors that may be exhibited by granular flows remains incomplete and there is no widely accepted constitutive law for the internal stresses developed by these flows. However, we may simplify the depth-averaged equations by invoking two further assumptions. First, we assume that the ratio of the shear to normal stresses is small ($p_{xx}, p_{yy} \gg p_{xy}$) and that to leading order the normal stresses are equal, $p_{xx}=p_{yy}=p_{zz}$.[12] This diverges from the approach of Savage and Hutter,[4] who introduced an earth pressure coefficient that measures the ratio

p_{xx}/p_{zz} and is different from unity. However, normal stress differences have been found to be small in simulations[22] and both Pouliquen and Forterre[20] and Gray *et al.*[12] suggest that for chute flows they should be neglected. We will demonstrate below that the inclusion of an earth pressure coefficient weakens the agreement between the experimental results and the theoretical model. Thus we find that the steady governing equations are given by

$$\frac{\partial}{\partial x}(hu) + \frac{\partial}{\partial y}(hv) = 0, \tag{5}$$

$$\frac{\partial}{\partial x}(u^2 h) + \frac{\partial}{\partial y}(uvh) + \frac{\partial}{\partial x}\left(\frac{g\cos\theta h^2}{2}\right) = -\frac{\tau_x}{\rho} + gh\sin\theta, \tag{6}$$

$$\frac{\partial}{\partial x}(uvh) + \frac{\partial}{\partial y}(v^2 h) + \frac{\partial}{\partial y}\left(\frac{g\cos\theta h^2}{2}\right) = -\frac{\tau_y}{\rho}. \tag{7}$$

With the exception of the drag and downslope acceleration terms on the right-hand side of (6) and (7), these equations are equivalent to those that express mass and momentum conservation for the steady flow of a polytropic gas with index 2.[23] Furthermore, they are identical to the shallow-water equations used to model hydraulic phenomena.[24]

We consider a uniform channelized flow, upstream of an obstacle, that is purely downslope $[\mathbf{u}=(U_1,0)]$ and of depth h_1. A constant flow depth and velocity are possible if the basal drag τ_x is equal to the downslope gravitational force $(\rho g h_1 \sin\theta)$. As will be discussed below, we found that the flows in the experiments reported here adjusted rapidly to these uniform conditions. We introduce dimensionless variables by scaling velocities by U_1, lengths by h_1, and stresses by ρU_1^2, and henceforth will assume that variables are dimensionless, unless indicated otherwise. An important dimensionless parameter is the upstream Froude number F which is given by

$$F^2 = \frac{U_1^2}{g h_1 \cos\theta}. \tag{8}$$

This is equivalent to the Mach number in gas flows and measures the speed of the flow relative to the speed of the small amplitude surface waves. In these experiments, and more generally for snow avalanches, $F \gg 1$. For example, Issler[2] suggests that for dry-snow avalanches, F lies between 5 and 10.

The system of governing equations (5)–(7) admits discontinuous solutions (shocks), across which the velocity and height of the flow may change abruptly. For stationary shocks, conservation of mass and momentum across the discontinuity is enforced through the following jump conditions:

$$[h\mathbf{u}\cdot\mathbf{n}]_-^+ = 0, \tag{9}$$

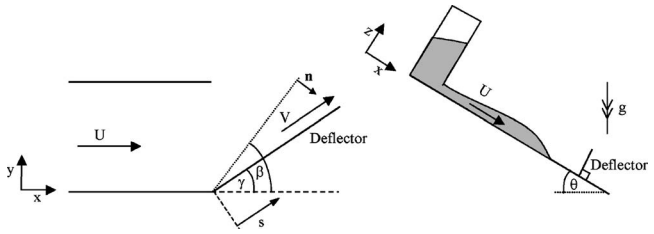

FIG. 1. The flow configuration in plan and side views.

$$\left[h\mathbf{u}(\mathbf{u}\cdot\mathbf{n}) + \frac{1}{2F^2}h^2\mathbf{n}\right]_-^+ = 0, \tag{10}$$

where $\mathbf{n}$ is a unit vector that is locally normal to the shock and $[\cdots]_-^+$ denotes the change in magnitude across the discontinuity. Note that downslope acceleration and drag do not affect these jump conditions, which in the spirit of this shallow-water model are idealized to be abrupt changes between the flow states. Further note that in the vicinity of the shock, the horizontal lengthscale of the flow may no longer exceed the vertical lengthscale. Thus, there may be significant vertical accelerations and the normal stress p_{zz} may no longer adopt a hydrostatic distribution. However, as in many hydraulic models, we assume that the adjustment between the states occurs over a sufficiently small distance so that we may treat it as a discontinuity.

Oblique shock

We now consider the deflection of the uniform downslope flow with dimensionless velocity, $\mathbf{u}=(1,0)$, and flow depth, $h=1$, by an impermeable, rigid barrier, orientated at an angle γ to the oncoming flow (see Fig. 1 and Sec. III). As described below, we find that a steady solution may be derived where the flow undergoes an abrupt transition in flow states via an "attached" shock, which originates from the junction of the barrier and the lateral channel wall and which is orientated at an angle β to the direction of steepest descent such that $\beta > \gamma$. Such a transition is analogous to the polar shock, which is widely reported in studies of gas dynamics, although the relationships on either side of the discontinuity are different since gas flows also conserve enthalpy.[23]

To analyze this transition we assume that immediately downstream of the shock the motion is tangential to the barrier, so that the velocity field may be written as $\mathbf{u}=(V\cos\gamma, V\sin\gamma)$. In contrast to gas dynamics, the granular flows may develop spatially downstream of the shock due to the action of gravity and drag. However for the experiments described below, the maximum distance between the shock and the barrier is sufficiently small so that the flow is unable to develop significantly and thus the assumption that it is parallel to the barrier is reasonable. We may thus employ the three jump conditions (9) and (10) to determine the speed V, and the flow depth H downstream of the shock, and the shock angle β, as functions of the upstream Froude number and the angle of the deflector.

The jump condition for conservation of mass implies that

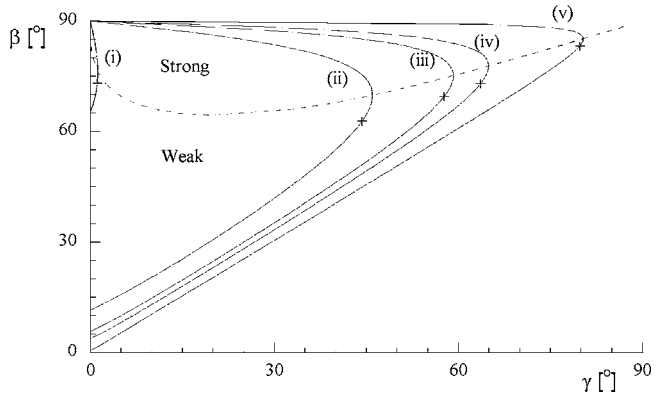

FIG. 2. The shock angle β as a function of the deflector angle γ for (i) $F=1.1$, (ii) $F=5$, (iii) $F=10$, (iv) $F=15$, and (v) $F=100$. Note that for each γ and F there are two shock angles, termed the "weak" and "strong" shocks; the dashed line (- - - -) indicates the boundary between these shocks and the locus of the maximum deflector angle γ_m. Also plotted on each curve (+) are the values of the deflector angle γ_f at which the flow downstream becomes critical.

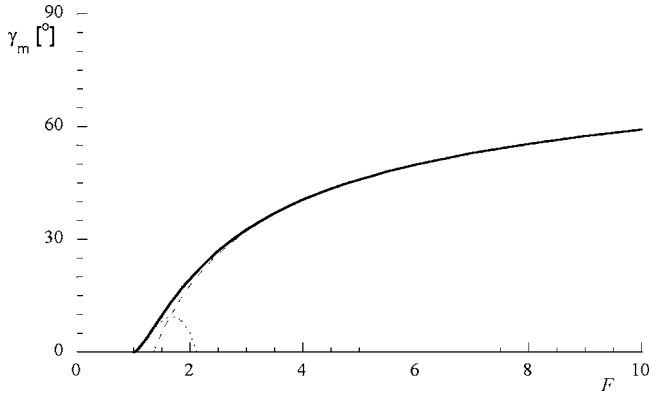

FIG. 3. The maximum angle of the deflector, γ_m, for which there is an attached shock as a function of the Froude number F (—) . Also plotted are the asymptotic representations of γ_m in the regimes $F \gg 1$ (- - -) and $0 < F-1 \ll 1$(-·-·-).

$$\sin\beta = HV\sin(\beta-\gamma), \tag{11}$$

while the conditions for the conservation of momentum yield

$$\sin^2\beta + \frac{1}{2F^2} = HV^2\sin^2(\beta-\gamma) + \frac{H^2}{2F^2}, \tag{12}$$

$$\cos\beta\sin\beta = HV^2\cos(\beta-\gamma)\sin(\beta-\gamma). \tag{13}$$

These may be solved simultaneously to give

$$\tan\gamma = \frac{4\sin\beta\cos\beta(1-F^2\sin^2\beta)}{-3+4\cos^2\beta(1-F^2\sin^2\beta)-\sqrt{1+8F^2\sin^2\beta}}. \tag{14}$$

We plot β as a function of γ for various values of the Froude number in Fig. 2. We note several features of this relationship. First, for a given Froude number and angle of deflector, we find that there are two possible shock angles, termed as the "weak" and "strong" shocks for the smaller and larger angles, respectively. Also, we find that the shock angle is bounded such that $\pi/2 \geqslant \beta \geqslant \sin^{-1}(1/F)$; in the absence of a deflector ($\gamma=0$), we may have a shock that is normal to the flow ($\beta=\pi/2$) and one which is at an angle $\sin^{-1}(1/F)$, across which the velocity and depth are continuous, but their spatial gradients are discontinuous. (In the context of gas dynamics, this is known as a Mach line.) In addition, we observe that there is a maximum angle of deflector γ_m for which there is an attached shock. At deflector angles greater than this ($\gamma > \gamma_m$), the shock is detached and located upstream of the junction between the channel and the deflector and may be curved (cf. the work by Chapman[23]). We plot γ_m as a function of the upstream Froude number in Fig. 3. Finally, we note that solutions for an attached shock may only be constructed when the upstream flow is supercritical ($F>1$).

It is also possible to derive relatively simple expressions for the dimensionless velocity, depth, and Froude number of the flow downstream of the shock . These are given as functions of β, γ, and F by

$$V = \frac{\cos\beta}{\cos(\beta-\gamma)}, \tag{15}$$

$$H = \frac{\tan\beta}{\tan(\beta-\gamma)}, \tag{16}$$

$$\hat{F} \equiv \frac{FV}{\sqrt{H}} = \frac{F\cos\beta}{\cos(\beta-\gamma)}\sqrt{\frac{\tan(\beta-\gamma)}{\tan\beta}}. \tag{17}$$

For strong shocks, the downstream flow is always subcritical ($\hat{F}<1$). For weak shocks, the flow is supercritical apart from for a small range of deflector angle $\gamma_f < \gamma < \gamma_m$. (In Fig. 2 we mark the change from supercritical to subcritical conditions.) We plot the difference between the shock and deflector angles ($\beta-\gamma$) and the ratio of the depths of the flows either side of the shock (H) as functions of the upstream Froude number and the deflector angle (Fig. 4). We note that for relatively high Froude numbers, the difference between the shock and deflector angles is only a weak function of the deflector angle.

We now analyze the relationships across the shock in the regime of high Froude numbers ($F \gg 1$), since this is applicable to the experiments reported below and natural-scale avalanches. First, the maximum angle, for which an attached shock may be found, is given by

$$\gamma_m = \frac{\pi}{2} - \frac{2^{3/4}}{F^{1/2}} - \frac{2^{1/4}}{6F^{3/2}} + O\left(\frac{1}{F^{5/2}}\right). \tag{18}$$

Also, flow downstream of a weak shock is subcritical when $\gamma > \gamma_f$, which in this regime is given by

$$\gamma_f = \frac{\pi}{2} - \frac{3\times 2^{1/2}}{2F^{1/2}} + O\left(\frac{1}{F^{5/2}}\right). \tag{19}$$

Finally, provided $F\cos\gamma \gg 1$, we find that

$$\beta - \gamma = \frac{2^{1/2}}{2F\cos\gamma} + O\left(\frac{1}{F^2}\right). \tag{20}$$

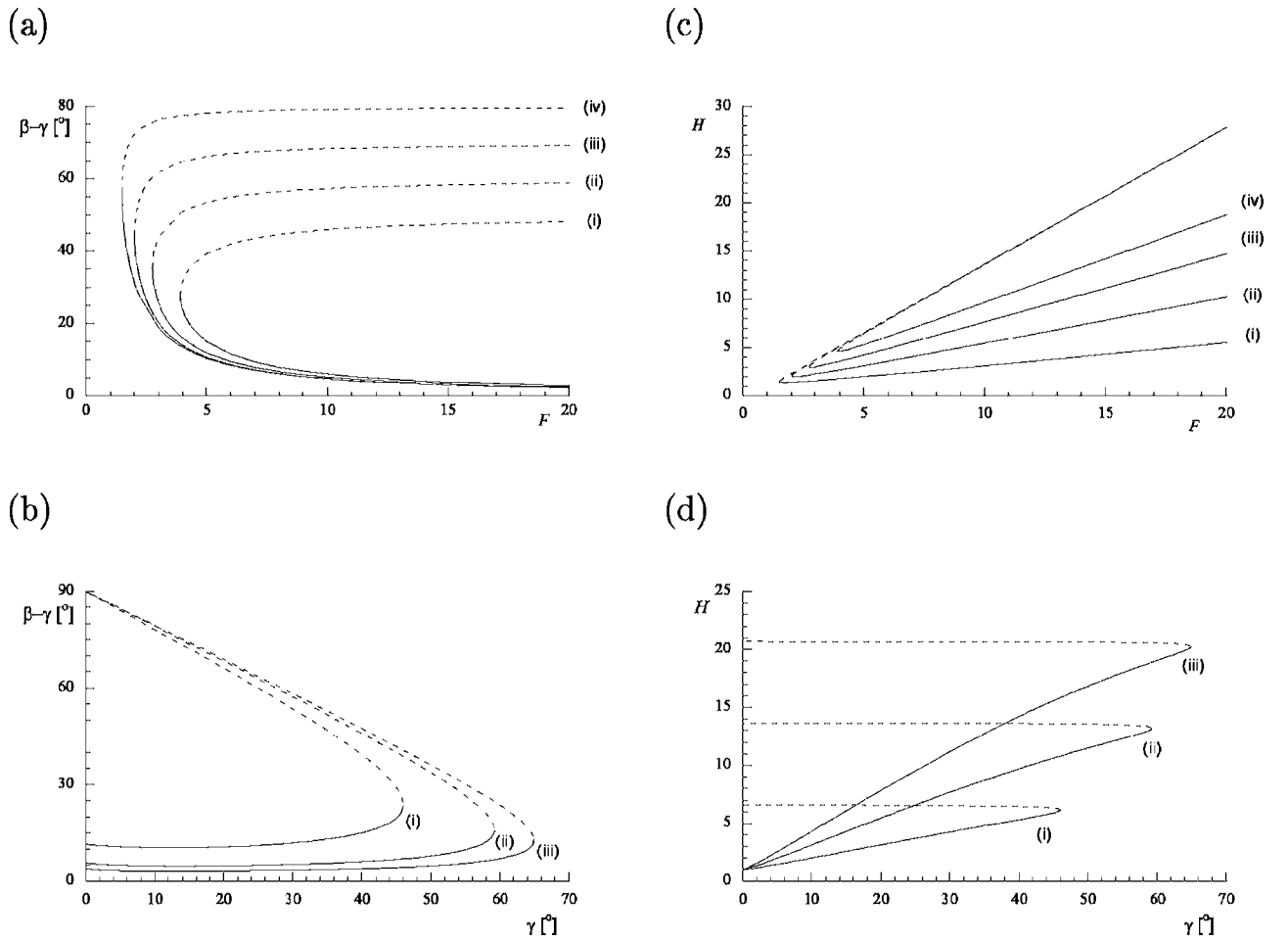

FIG. 4. (a) The difference between the shock and deflector angles, $\beta-\gamma$, as a function of the Froude number F for (i) $\gamma=10°$, (ii) $\gamma=20°$, (iii) $\gamma=30°$, and (iv) $\gamma=40°$. (b) The difference between the shock and deflector angles, $\beta-\gamma$, as a function of the deflector angle γ for (i) $F=5$, (ii) $F=10$, and (iii) $F=15$. (c) The ratio of the upstream and downstream depths of the flow, H, as a function of the Froude number F for (i) $\gamma=10°$, (ii) $\gamma=20°$, (iii) $\gamma=30°$, and (iv) $\gamma=40°$. (d) The ratio of the upstream and downstream depths of the flow, H, as a function of the deflector angle γ for (i) $F=5$, (ii) $F=10$, and (iii) $F=15$. In each figure the weak shock is plotted with a solid line (—) and the strong shock with a dashed line (- - - -) .

We may also analyze the properties of the flows for which the upstream Froude number only just exceeds unity $(0<F-1\ll 1)$. In this regime we find that

$$\gamma_m=\frac{8\times 6^{1/2}}{27}(F-1)^{3/2}-\frac{190\times 6^{1/2}}{729}(F-1)^{5/2}+O[(F-1)^{7/2}], \tag{21}$$

$$\gamma_f=\tfrac{2}{3}(F-1)^{3/2}-\tfrac{31}{54}(F-1)^{5/2}+O[(F-1)^{7/2}]. \tag{22}$$

III. EXPERIMENTS

A. Experimental procedure

We conducted three series of experiments to investigate the deflection of rapid free-surface flows by oblique obstacles. For two of the series, the flow consisted of small, dry, glass beads while for the third, sustained flows of water were generated. In each experiment, the material was released at the top of an inclined chute and flowed rapidly downslope towards a deflecting dam placed in the chute at an angle γ between 0° and 40° to the oncoming flow (see Fig. 1). The deflector was sufficiently high so that none of the flow overtopped it. Measurements of the flow speed and depth were taken from video footage of the motion and from an optical distance sensor that employed reflections of infrared light to determine distances. Particular attention was paid to the steady depth profile of the flow on the dam (the "run-up") and to the initial interaction between the flow and the dam. The experimental conditions are summarized in Table I.

The rapid granular flows employed dry, glass beads (ballotini), which were almost spherical and of mean size 90 μm and particle density 2500 kg m^{-3}. The bulk density of this material is $\approx$1600 kg m^{-3}. The flows were generated by rapidly removing a lockgate behind which the beads were initially placed. For series I, the opening was constricted to control the flow depth at the source; the opening was not constricted for series II. The particles flowed down an inclined wooden plane with a dynamic friction angle of $\approx$20°, which is just smaller than the measured internal friction angle of the particles. The grains flowed within a channel which was of width 0.1 m and 0.325 m in series I and II, respectively. The deflectors were also made of wood and were located 1.7 m from the source. For most of the experiments, the upstream face of the deflecting dam was normal to

TABLE I. The experimental conditions for the three series, I, II, and III. For each chute inclination, a number of runs were carried out with dams at different deflecting angles ($\gamma = 8° - 44°$). In each run the flow speed and depth upstream of the obstacle were remeasured; the values given in this table are indicative of those measured.

Series	Material	Incline (deg)	Flow speed ($m\ s^{-1}$)	Flow depth (mm)	Froude number
I	Ballotini	26.5±0.5	0.7±0.01	2.0±0.2	5
	Ballotini	30.3±0.5	1.85±0.07	2.7±0.2	12
	Ballotini	30.3±0.5	1.52±0.05	1.3±0.2	14
II	Ballotini	38±0.5	3.5±0.1	9.0±1	13
III	Water	3	0.95±0.05	5.5±0.5	4.1
	Water	6	1.18±0.07	4.5±0.5	5.6
	Water	9	1.25±0.08	4.0±0.5	6.4

the base of the inclined chute, although for a few runs the upstream face was tilted backwards. As discussed below this appeared to make little difference to the steady deflection patterns.

The granular material accelerated rapidly upon release to attain a steady speed and flow depth within 0.5 m of the source. In series I, the motion was maintained for ≈20 s; in contrast, series II was of much shorter duration, lasting just under 2 s. These latter flows consisted of a short agitated and relatively dilute front, followed by a slightly slower and denser main body and a much slower tail. Such features are reminiscent of Boussinesq gravity currents,[25] natural-scale snow avalanches,[2] and ping-pong ball avalanches.[26] For series II, our measurements of the deflection were taken during the interaction of the interior, main body of the flow.

Experiments were also conducted with rapid flows of water. For this series, water is supplied to a reservoir, flows over a weir and under a partially raised gate into an inclined channel of width 0.2 m. This configuration was found to significantly reduce unsteadiness and wave action and to result in a uniform flow down the inclined plane. The flow was deflected by a perspex dam that was located 0.7 m downslope from the reservoir. The Reynolds number in these experiments was calculated to be ≈5000, which is sufficiently high so that viscous effects may be neglected.

B. Experimental results

Upon impacting the deflector, the flows rapidly adjusted to a state in which an oblique shock could be clearly identified. The structure and form of the shock was relatively steady. Figure 5 provides photographic images of the shocks that formed in the experiments with granular and water flows. We first compare the experimental measurements and theoretical predictions of the bulk features of the flow before describing the initial impact in greater detail (Sec. III C).

In Fig. 6(a) the experimentally measured difference between the angle of the oblique shock and the deflector, $\beta - \gamma$, is compared with the theoretically calculated value, which is derived from (14). The data in Fig. 6(a) comprise all the experimental series, and the error bars on the theoretically calculated angles arise primarily from the error in measuring accurately the depth of the rapid flow and thus determining the upstream Froude number. In some experiments, the relative error in this measurement may be up to 10% of the total flow depth. We note that there is good agreement between the theoretical calculations and the experimental measurements.

We also compare measurements of the depth of the flow at the deflecting dam, downstream of the shock, relative to the upstream depth H with the theoretical predictions in Fig. 6(b). As is discussed further below, the flow depth does not change abruptly; instead there is an adjustment zone within which the depth varies. For the purposes of this figure, we average the flow depth along the dam, noting that in most cases the adjustment zone is relatively short. We find again that there is good agreement between the theory and the experiments.

Some experiments were conducted with deflecting dams, which had upstream faces that were at less than 90° to the base of the chute. It was observed that these tilted dams did not affect the structure of the flow. Similar shock angles and depth profiles along the dams were observed, indicating that the transition between flow states occurs significantly upstream of the dam and is not affected by the inclination of its front face.

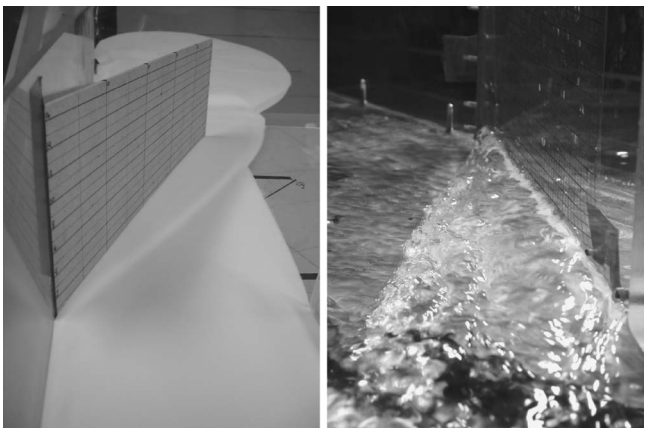

FIG. 5. Photographs of oblique shocks in a granular flow (series I, looking downstream onto the deflector) and a water flow (series III, looking upstream into the flow along the deflector) with upstream Froude numbers 5 and 4.5 and deflector angles of 24° and 20°, respectively.

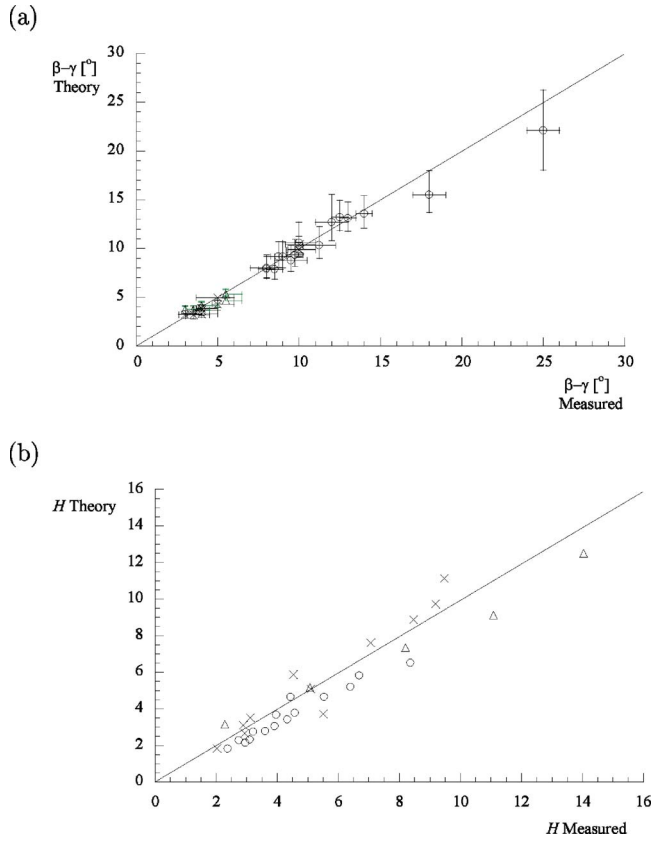

FIG. 6. Predicted values of (a) $\beta-\gamma$ and (b) H plotted against the experimentally measured values for series I (×), II (△), and III (○). The solid lines denote perfect agreement.

We note that our results are somewhat different from those of Gray *et al.*,[12] even though they are analyzed using the same framework for modeling. Gray *et al.*[12] reported a single experiment for which the upstream Froude number is 5.79 and the deflector is at an angle of 25° to the flow direction. For such conditions and using (14), we evaluate the shock angle β to be 34°. This value differs from the calculation of Gray *et al.*,[12] because they did not explicitly use condition of the continuity of the tangential velocity across the shock (15). Rather, they calculated the shock angle as a function of the downstream relative depth H and the upstream Froude number F, and using their measured values they found that β is 29.04°. This contrasts with the analysis developed in this study, which determines H as a part of the solution in terms of F and γ. Indeed, all downstream and shock conditions, H, V, and β, may be evaluated in terms of the upstream flow. It is intriguing, however, that their calculated angle is close to their experimentally measured angle of 29°. It is also intriguing that in our study we have one experimental run with conditions quite close to those reported by Gray *et al.*,[12] namely, $F=5.3$ and $\gamma=25°$. For this experiment we measure a shock angle of 35°. There are a number of differences between the experiment of Gray *et al.*[12] and the experimental series reported here. Not only were different materials employed for both the flowing particles and the base and sidewalls of the chute, but also the flows were of different durations; indeed it may be that the relatively short-lived experiments of Gray *et al.*[12] were not in a steady state. Additionally, their measurement of the depth of the upstream flow, which was reported to be ≈4 mm, may be subject to significant variability, given that the particles were of size 1 mm and thus the flows were on average just four particles thick. Uncertainties in this measurement have a large effect on the magnitude of the upstream Froude number.

The good agreement between the theoretical predictions and our experimental measurements, as shown in Figs. 6(a) and 6(b), suggests that the shallow water framework is appropriate for modeling rapid granular flows and their interaction with oblique deflectors. In particular, the theoretical predictions were based upon the assumption that the normal stress was isotropic. We note that some models of shallow granular flows permit normal stress differences ($p_{xx}/p_{zz}=K\neq 1$); Savage and Hutter[4] treat the flowing material as a cohesionless continuum and assume that the frictional contacts between particles follow Mohr-Coulomb behavior. In this case, the ratio K is a function of the internal angle of friction for the material and the friction angle for the sliding motion between the particulate and the chute. This formulation admits two values for K depending on whether the material is in an "active" ($\partial u/\partial x>0$) or "passive" ($\partial u/\partial x<0$) state.[4] These experiments, with measured internal and basal friction angles of 21° and 20°, respectively, yield $K=1.03$ for the active state and $K=1.55$ for the passive state. If an earth pressure coefficient with either of these values is introduced into the shock conditions, the agreement between the theory and the experiments is weakened, although only slightly so for the active stress state.

Finally, we note that although the particles employed in this investigation were relatively small, and hence may be susceptible to significant interactions with the interstitial fluid, such as "air" drag, our results demonstrate that an accurate model of the motion may be developed by neglecting these effects.

C. Initial interaction with the deflector

While the steady deflection of these rapid streams by oblique deflectors was similar for both granular and water flows, the character of their initial impacts differed. The granular flows rapidly established a steady profile along the dam and were not observed to splash appreciably higher than the height predicted by the shock conditions. In contrast, the water flows were observed to run up the dams considerably higher than the predicted height. This initial interaction was short lived at each location on the dam, typically lasting just 20 ms, which corresponds to one frame of the video recording, although the evolution of the splash along the dam face could be readily followed.

A naive estimate of the height of these splashes in the experiments with water can be made by applying Bernoulli's theorem to streamlines at the free surface and assuming that the component of velocity normal to the obstacle vanished and is compensated by an increase in flow depth. Thus the height relative to the upstream flow depth should be $1+F^2\sin^2\gamma/2$. However, this form of Bernoulli's theorem takes no account of the violent interaction with the dam and is significantly lower than the measured heights. Following

Cooker and Peregrine,[27] we hypothesize that during the initial interaction, the velocity normal to the dam is suppressed over a very short time scale and this is balanced by a substantial increase in the pressure. Then integrating the governing equation of motion over a short period from immediately before to immediately after the impact yields the dominant balance

$$\mathbf{u}_a - \mathbf{u}_b = -\frac{1}{\rho}\nabla P, \tag{23a}$$

where

$$P(\mathbf{x}) = \int_{t_b}^{t_a} p \, \mathrm{d}t. \tag{23b}$$

In this expression, $P(\mathbf{x})$ is the pressure impulse and $\mathbf{u}_b$ and $\mathbf{u}_a$ are the velocities before and after the impact, respectively. Cooker and Peregrine[27] argue that the other terms in the governing equation are negligible. For water, the motion is incompressible and thus the pressure impulse satisfies Laplace's equation ($\nabla^2 P=0$). This is a crucial difference between the impact of water and that of granular materials. Granular flows may develop equally high dynamic pressures on impact, but the effects of their compressibility lead to lower vertical velocities and, consequently, lower splash heights.

We may estimate the pressure impulse in these flows by analyzing the idealized problem of a flat fronted flow impacting a vertical wall, which follows an example presented by Cooker and Peregrine.[27] Solving Laplace's equation permits the velocity of the free surface, $\mathbf{u_a}=(u_a, w_a)$, relative to the upstream flow speed, to be deduced after the impact. Cooker and Peregrine[27] show that

$$u_a(\hat{x}) = \sin\gamma, \quad w_a(\hat{x}) = -\frac{2\sin\gamma}{\pi}\log\left[\frac{\pi\hat{x}}{4}\right] \quad \text{when } \hat{x} \ll 1, \tag{24}$$

where $\hat{x}$ is the distance upstream of the obstacle, normal to the dam. This does not apply at the wall ($\hat{x}=0$), because friction regularizes the singularity in the velocity field. Nevertheless, we note that the impact and the increase in the pressure lead to a large vertical velocity that is capable of sending a jet up the dam. Assuming that the vertical velocity of the jet is given by this velocity field at $\hat{x}=d$, a revised estimate of the height of the initial splash is given by

$$1 + \frac{F^2\sin^2\gamma}{2}\left[1 + \frac{4}{\pi^2}\log^2\left(\frac{\pi d}{4}\right)\right]. \tag{25}$$

Cooker and Peregrine[27] do not provide a means for assessing the magnitude of d. In these experiments we measured the height of the splash for a range of deflector angles. Thus we chose d to take the value which makes this estimate accurate for $\gamma=\pi/2$. This yields $d=0.29$, which corresponds to $w_a \approx u_a$ and a dimensional distance of 3 mm. We use this value to calculate the splash heights for all other deflector angles and we note from Fig. 7 that this provides a reasonable estimate of the measured heights.

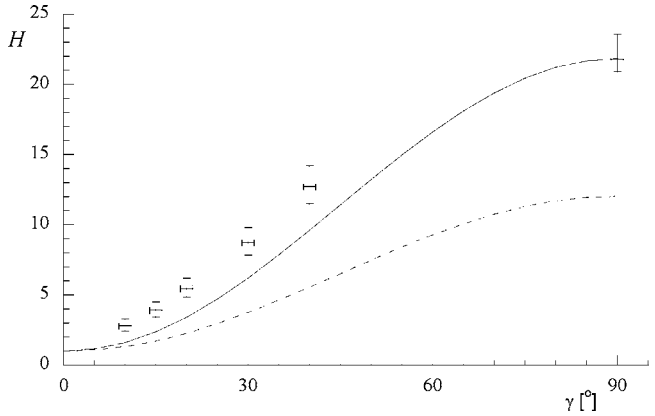

FIG. 7. The experimentally measured splash height as a function of the angle of the deflector. Also plotted are the predictions from the pressure impulse theory (—) and from a naive use of Bernoulli's theorem (- - - -) .

D. Flow development

After the initial interaction, the flow developed steady profiles along the dams for all the deflector angles for which there was an attached shock. However, the flow depths did not adjust immediately to the depths predicted by the shock theory (see Fig. 8); rather, the flow depth along the dam increased almost monotonically from the intersection of the

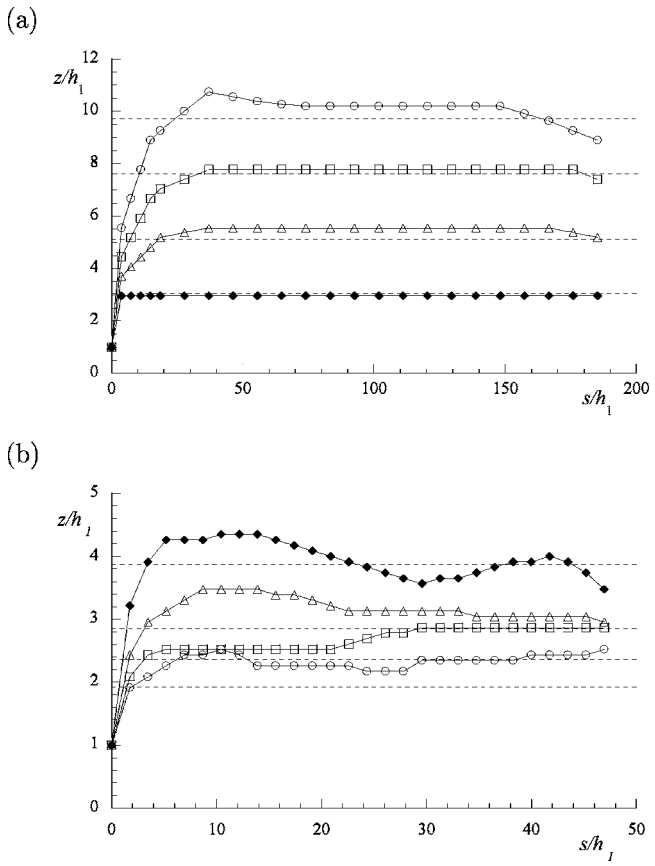

FIG. 8. The dimensionless height of the flow along the dam, z/h_1, as a function of the dimensionless distance along the dam, s/h_1, for (a) granular flows with $\gamma=8°$, 15° ,24°, and 32 ° and $F=12$; and (b) water flows with $\gamma=10°$,15°, 20°, and 30 ° and $F=4.5$. Also plotted are the predictions of the steady depth from the shock conditions (- - - -) .

dam and the channel boundary towards the steady-state condition. The origin of this spatial development may be readily explained and is the oblique-shock counterpart of the spatial development of hydraulic jumps for which the flow undergoes a transition between the two flow states over a finite distance (see, for example, the work by Hager[28]). We estimate that the distance parallel to the chute base and normal to the shock, over which the transition occurs, is proportional to the difference in flow depths upstream and downstream of the shock, $H-1$. Thus the distance along the dam before the steady-state height is attained is proportional to $(H-1)/\tan(\beta-\gamma)$, which in the regime $F \gg 1$ is approximately given by $F^2 \sin(2\gamma)$. We note from Fig. 8, and from other experimental results, that the adjustment distance along the dam does increase with increasing values of both F and γ and that this is consistent with the preceding argument.

IV. CONCLUSIONS

In this study, we have measured the deflection of free-surface, downslope flows of water and granular materials and have shown the existence of oblique shocks across which the velocity and the depth of the flow changes almost discontinuously. We have also demonstrated that the shallow-water framework provides a good model for predicting the angle of the weak attached shock and the dimensionless flow depth downstream of the shock as a function of the upstream Froude number F and the angle of the deflecting dam. The quantitative agreement between the theory and the observations suggests that there are no normal stress differences within these granular flows (i.e., the normal stresses are isotropic). Furthermore, in these rapidly flowing shallow states they adopt a hydrostatic distribution in which the vertical gradient of p_{zz} balances the weight of the mobile layer. In analyzing these oblique shocks using this depth-averaged formulation, we have not had to make any assumptions about the dependence of the shear stress upon the flow speed, density, or degree of agitation, because the jump conditions are applied over an infinitesimal control volume. We have assumed, however, that the flow is incompressible—but this is not such a strong assumption under the conditions examined here, where the shock separates two rapidly flowing regions $(F, \hat{F} \gg 1)$ within which the entire flow depth is mobilized and for which it is plausible that the bulk density does not vary strongly. A more complete model could be formulated in which variations in bulk density and energy across the shock were also accounted for, but this does not appear to be necessary for these flows.

It is also interesting to note that the experiments with water and with grains yield similar results when they attain their steady states. We find substantial differences in the behavior of the initial interaction with the obstacle; we find that the water splashes up much higher. We ascribed this difference to the incompressibility of water, which led to high transient pressures developing and consequently a rapid acceleration of a water jet up the face of the dam. The granular flows did not exhibit such a phenomenon, and we note that the flow front was dilute and able to compress considerably.

Snow avalanches pose significant natural hazards and dams have been used to deflect them away from inhabited regions. An interesting example occurred at Flateyri, western Iceland, in 1999, when an avalanche of approximate volume 10^5 m^3 hit a deflecting dam located above the village. The dam had been designed to deflect an avalanche by $\approx 20°$. Observations of the avalanche debris left by the motion suggest that an oblique shock was formed during the interaction between the dam and the flow.[29] The deposited debris showed that the impact had channelized a part of the avalanche into a thicker stream, which traveled parallel to the dam and formed an angle of $\approx 5°$ with the dam face. The magnitude of this shock angle coincides with the predictions of the theory developed here if the upstream Froude number of the avalanche were close to 10—and this concurs with the published estimate of the Froude number of the avalanche.[29] The jump conditions also predict a fivefold depth increase across the oblique shock. This is, however, an underprediction of the observed run-up on the dam if the upstream depth of the avalanche was correctly estimated to be 1 m (Ref. 29) and if the highest marks on the dam indicate the run-up of the dense bulk of the flow, rather than splashing, or the saltation layer.[2]

The experimental observations presented here are important indications of the dynamical and mechanical properties of granular avalanches. The shallow-water theory and the deviations from it provide a starting point for more realistic theoretical descriptions of rapid granular flows. Furthermore, the results may be directly applied to formulate new design criteria for deflecting dams. Importantly, this shock theory, confirmed by laboratory experiment, can predict the deflection angle as a function of the angle that the deflector makes to the oncoming flow and of the upstream Froude number. Also, the theory establishes the maximum angle of the deflector at which an attached shock occurs. This may be important for the design of deflecting barriers; if too large a deflection is sought then the shock is detached from the barrier and the flow structure is significantly different. Finally, we remark that this study has further underlined the importance of resolving shocks in numerical computations of rapid granular flows, such as snow avalanches.

ACKNOWLEDGMENTS

The authors gratefully acknowledge many fruitful discussions with Tomas Jóhannesseon and Dieter Issler and financial support from the Icelandic Research Fund for Graduate Students, the University of Bristol, the Icelandic Avalanche Fund, and the SATSIE research project (EU Contract No. EVG1-CT2002-00059).

[1] W. B. Dade and H. E. Huppert, "Long runout rockfalls," Geology **26**, 803 (1998).
[2] D. Issler, "Experimental information on the dynamics of dry-snow avalanches," in *Dynamic Response of Granular and Porous Materials under Large and Catastrophic Deformations*, edited by K. Hutter and N. Kirchner (Springer, Berlin, 2003), pp. 109–160.
[3] R. Behringer, H. Jaegar, and S. Nagel, "Introduction to the focus issue on granular materials," Chaos **9**, 509 (1999).
[4] S. B. Savage and K. Hutter, "The motion of a finite mass of granular material down a rough incline," J. Fluid Mech. **199**, 177 (1989).
[5] P. C. Johnson, P. Nott, and R. Jackson, "Frictional-collisional equations of

motion for particulate flows and their application to chutes," J. Fluid Mech. **210**, 501 (1990).
[6]O. Pouliquen, "Scaling laws in granular flows down rough inclined planes," Phys. Fluids **11**, 542 (1999).
[7]S. Horlück and P. Dimon, "Grain dynamics in a two-dimensional granular flow," Phys. Rev. E **63**, 031301 (2001).
[8]E. C. Rericha, C. Bizon, M. D. Shattuck, and H. L. Swinney, "Shocks in supersonic sand," Phys. Rev. Lett. **88**, 014302 (2002).
[9]A. Samadani, L. Mahadevan, and A. Kudrolli, "Shocks in sand flowing in a silo," J. Fluid Mech. **452**, 293 (2002).
[10]S. B. Savage, "Gravity flow of cohesionless granular materials in chutes and channels," J. Fluid Mech. **92**, 53 (1979).
[11]C. E. Brennen, K. Sieck, and J. Paslaski, "Hydraulic jumps in granular material flow," Powder Technol. **35**, 31 (1983).
[12]J. M. N. T Gray, Y. C. Tai, and S. Noelle, "Shock waves, dead zones and particle-free regions in rapid granular free-surface flows," J. Fluid Mech. **491**, 161 (2003).
[13]R. Ocone and G. Astarita, "Compression and rarefaction waves in granular flow," Powder Technol. **82**, 231 (1995).
[14]A. Goldshtein, M. Shapiro, L. Moldavsky, and M. Fichman, "Mechanics of collisional motion of granular materials. Part 2. Wave propagation through vibrofluidized granular layers," J. Fluid Mech. **287**, 349 (1995).
[15]A. Kamensetsky, A. Goldshtein, M. Shapiro, and D. Degani, "Evolution of a shock wave in a granular gas," Phys. Fluids **12**, 3036 (2000).
[16]C. R. Wassgren, J. A. Cordova, R. Zenit, and A. Karion, "Dilute granular flow around an immersed cylinder," Phys. Fluids **15**, 3318 (2003).
[17]D. McClung and P. Schaerer, *The Avalanche Handbook* (The Mountaineers, Seattle, 1993), p. 287.
[18]K. M. Hákonardóttir, A. J. Hogg, J. Batey, and A. W. Woods, "Flying avalanches," Geophys. Res. Lett. **30**, 2191 (2003).
[19]K. M. Hákonardóttir, A. J. Hogg, T. Jóhannesson, and G. G. Tomasson, "A laboratory study of the retarding effect of braking mounds," J. Glaciol. **49**, 191 (2003).
[20]O. Pouliquen and Y. Forterre, "Friction law for dense granular flows: application to the motion of a mass down a rough inclined plane," J. Fluid Mech. **453**, 133 (2002).
[21]A. J. Hogg and D. Pritchard, "The effects of drag on dam-break and other shallow inertial flows," J. Fluid Mech. **501**, 179 (2004).
[22]D. Ertas, G. S. Grest, T. C. Halsey, D. Levine, and L. E. Silbert, "Gravity-driven dense granular flows," Europhys. Lett. **56**, 214 (2001).
[23]C. J. Chapman, *High Speed Flow* (Cambridge University Press, Cambridge, 2000), p. 258.
[24]G. B. Whitham, *Linear and Nonlinear Waves* (Wiley, New York, 1974), p. 636.
[25]J. E. Simpson, *Gravity Currents in the Environment and the Laboratory* (Cambridge University Press, Cambridge, 1997), p. 244.
[26]J. McElwaine and K. Nishimura, "Ping-pong ball avalanche experiments," in *Particulate Gravity Currents*, Special Publication Number 31 of the International Association of Sedimentologists, edited by B. McCaffrey, B. Kneller, and J. Peakall (Blackwell Science, London, 2001), p. 135.
[27]M. J. Cooker and D. H. Peregrine, "Pressure-impulse theory for liquid impact problems," J. Fluid Mech. **297**, 193 (1995).
[28]W. H. Hager, *Energy Dissipators and Hydraulic Jumps* (Kluwer Academic, Dordrecht, 1992).
[29]T. Johannesson, "Run-up of two avalanches on the deflecting dams at Flateyri, northwestern Iceland," Ann. Glaciol. **32**, 350 (2001).